Differential activation of spinal cord glial cells in murine models of neuropathic and cancer pain.

Hald, Andreas; Nedergaard, S; Hansen, RR; Ding, Ming; Heegaard, AM

Published in:
European Journal of Pain

DOI:
doi:10.1016/j.bone.2004.12.010

Publication date:
2009

Document Version
Publisher's PDF, also known as Version of record

European Journal of Pain 13 (2009) 138–145

Contents lists available at ScienceDirect

European Journal of Pain

journal homepage: www.EuropeanJournalPain.com

Differential activation of spinal cord glial cells in murine models of neuropathic and cancer pain

Andreas Hald [a], Signe Nedergaard [a], Rikke R. Hansen [a], Ming Ding [b], Anne-Marie Heegaard [a,*]

[a] Department of Pharmacology and Pharmacotherapy, Faculty of Pharmaceutical Sciences, Copenhagen University, Universitetsparken 2, 2100 Copenhagen, Denmark
[b] Department of Orthopaedics, Odense University Hospital, Odense, Denmark

ARTICLE INFO

Article history:
Received 3 November 2007
Received in revised form 26 February 2008
Accepted 31 March 2008
Available online 21 May 2008

Keywords:
Astrocytes
Microglia
Glia
Bone
Pain
Cancer
Neuropathic

ABSTRACT

Activation of spinal cord microglia and astrocytes is a common phenomenon in nerve injury pain models and is thought to exacerbate pain perception. Following a nerve injury, a transient increase in the presence of microglia takes place while the increased numbers of astrocytes stay elevated for an extended period of time. It has been proposed that activated microglia are crucial for the development of neuropathic pain and that they lead to activation of astrocytes which then play a role in maintaining the long term pathological pain sensation. In the present report, we examined the time course of spinal cord glial activation in three different murine pain models to investigate if microglial activation is a general prerequisite for astrocyte activation in pain models. We found that two different types of cancer induced pain resulted in severe spinal astrogliosis without activation of microglia. In contrast, sciatic nerve injury led to a transient activation of microglia and sustained astrogliosis. These results show that development of hypersensitivity and astrocyte activation in pain models can take place independent of microglial activation.

1. Introduction

Nerve injury or inflammation may lead to spontaneously evoked pain and hypersensitivity towards thermal or tactile stimuli (Baron, 2006). Pathological pain is associated with altered gene expression in both primary afferent neurons and second order spinal cord neurons (Ji et al., 2003; Lee et al., 2005). Furthermore, microglial activation, a hallmark of CNS pathologies involving neuronal damage or death, also occurs following injury to peripheral nerves. In the latter scenario, microglia are activated in spinal cord areas containing the fibers and cell bodies of the damaged nerve (Hald and Lotharius, 2005; Lin et al., 2007; Sweitzer et al., 1999). As inhibition of microglial activation blocks hypersensitivity following nerve injury and that intrathecal injection of activated microglia leads to hypersensitivity, microglia are thought to play a crucial role in neuropathic pain development (Hains and Waxman, 2006; Raghavendra et al., 2003; Coull et al., 2005). Microglial mediated sensitization may be induced through the release of nerve sensitizing factors such as brain derived neurotrophic factor, interleukin (IL)-1β, tumor necrosis factor (TNF)-α, nitric oxide (NO) and prostaglandins (Coull et al., 2005; Lin et al., 2007; Lund et al., 2006; Park et al., 2007; Raghavendra et al., 2003). Besides the proalgesic effect of microglial released substances, some of these substances are also capable of activating surrounding astrocytes that may result in the spinal astrogliosis found to correlate with hypersensitivity in neuropathic rats (Falsig et al., 2004; Raghavendra et al., 2003; Garrison et al., 1991). Activated astrocytes are speculated to enforce pain sensation through the expression of proalgesic cytokines and production of interglial communication networks (Hansson, 2006).

Stimulation of astrocyte cultures with neurotransmitters, released by primary afferent neurons, such as glutamate, substance P (SP), calcitonin gene related peptide (CGRP), ATP and NO induce astrocyte alterations mimicking those observed in animal pain models, including increased glial fibrillary acidic protein (GFAP) expression and changed morphology (Brahmachari et al., 2006; Lazar et al., 1991; Neary et al., 1994; Noble et al., 1992; Guo et al., 2007). Thus, besides the putative effect of activated microglia on adjacent astrocytes, the astrogliosis observed in pain models could also result from stimulation by neurotransmitters released from signaling nociceptors. This notion is supported by in vivo studies showing that the glutamate antagonist MK-801 abrogate pain induced astrogliosis, which emphasizes the role of astrocyte expressed glutamate receptors or interneuronal synaptic transmission, for astrocyte activation (Garrison et al., 1994).

In the present study, we investigated the temporal development of pain behavior and glial activation in two cancer pain models and a nerve injury pain model. All three models exhibited hypersensitivity and increased spinal GFAP expression while increased presence of microglia was restricted to the nerve injury model. Furthermore, GFAP expression along the spinal cord was analyzed

* Corresponding author. Tel.: +45 35336322; fax: +45 35336020.
E-mail address: amhe@farma.ku.dk (A.-M. Heegaard).

1090-3801/$34.00
doi:10.1016/j.ejpain.2008.03.014

and astrogliosis was found to span several segments both rostrally and caudally from the segments where the involved primary afferent neurons entered the spinal cord. These results demonstrate that activation of astrocytes in pain models can take place independent of microglial activation.

2. Materials and methods

2.1. Animals

All experiments were carried out on 6 week old C3H/HeN mice (M-B Taconic, Tornbjerg, DK). Animals were kept in a room with a 12 h light/dark cycle and were fed standard laboratory diet and tap water ad libitum. The experiments were approved by the Danish Committee for Experiments on Animals and conducted according to the guidelines of the International Association for the Study of Pain.

2.2. Cell line

NCTC-2472 (NCTC) cells obtained from the American Type Culture Collection (ATCC, CCL-11) were grown according to ATCC guidelines. Cultures were harvested when they were 80% confluent by exposure to calcium free PBS + 1 mM EDTA for 3 min and resuspended in α-MEM (Gibco, 22571-020) to a final concentration of either 10×10^6 or 50×10^6 cells/ml. Cells were kept on ice until use.

2.3. Surgeries

Animals were divided into three groups which underwent either a partial sciatic nerve ligation (PSNL) operation, an injection of NCTC cells into the right femoral bone marrow cavity or an injection of NCTC cells in close proximity of the sciatic nerve in the gluteal region. Two extra groups for investigation of astrogliotic spread were operated. One of these underwent bone cancer induction and the other a bone cancer sham operation.

PSNL was performed according to Malmberg and Basbaum (1998). Following anesthesia with Zoletil mix-50 (zolazepam 25 mg/ml, tiletamin 25 mg/ml, xylazin 20 mg/ml, butorphanol 10 mg/ml, KVL, Denmark), 2 μl/g body weight, the sciatic nerve was exposed through an incision on the back of the mice and approximately 1/2 of the nerve was tightly ligated with a 8–0 suture. The wound was closed by suturation.

Bone cancer bearing (BCB) mice were produced as previously described by Schwei et al. (1999) with some modifications. Briefly, mice were anesthetized with Zoletil mix-50, 2 μl/g body weight, and a small incision was made above the right knee. The patella ligaments were loosened from the surrounding tissue and the patella was gently pushed lateral to expose the femoral bone. A small hole projecting to the marrow cavity was drilled with a 30 gauge needle between the condyles and 100,000 NCTC cells in 10 μl α-MEM were injected. The hole was blocked with bone wax (Johnson & Johnson Intl, W810) and the area was thoroughly cleaned with saline and a cotton stick and the skin was ligated with wound clips (Appose 888 6803712, Autosuture, USA). Similar sham operations were performed with injection of α-MEM only.

Sciatic nerve proximal cancer (SNPC) was induced by injecting 100,000 NCTC cells in 2 μl α-MEM in the gluteal region using a method described by Shimoyama et al. (2005). Briefly, mice were anaesthetized with Zoletil mix-50, 2 μl/g body weight and the sciatic nerve was exposed through an incision on the lower back of the animal. Cells were injected in close vicinity of the sciatic nerve at the level of the trochanter and the wound was closed by suturation.

2.4. Behavioral tests

Each of the three operated groups was divided into three subgroups. Each subgroup was tested at distinct day(s) after which they were euthanized and prepared for histology. Groups consisting of BCB mice were tested once either on day 7, 14 or 17. SNPC groups were tested on either day 7 or 14, or on day 17 and 21. PSNL groups were tested on either day 7, 14 or 21. Before operations, pretests were performed on a mixed group of 10 mice belonging to different groups. The mice used for analysis of astrogliotic spread were tested every other day following day 14 and prepared for immunohistochemistry when reaching a limb use score of one or below (see next paragraph).

The animals' ability to use the affected leg was evaluated in open field limb use tests and tactile hypersensitivity was evaluated by von Frey monofilaments. In the limb use test, the animals were allowed to adapt for 10 min in a transparent empty animal cage (42.5×26.6 cm) after which the use of their right hind limb was observed for a 3 min period and graded on a continuous and linear scale from 0 to 4, where 0 designate no use of the affected limb and 4 normal use of limb.

Von Frey tests were performed with monofilaments supplying pressure from 0.008 to 2 g (North Coast Medical Inc., Morgan Hill, Ca, USA). The animals were allowed to acclimatize for 1 h before the test was performed. The mice were stimulated five times with each monofilament and three or more paw withdrawals were considered a positive response. The left paw functioned as an internal control for each mouse and a withdrawal threshold ratio, defined as the right paw withdrawal threshold divided by the left paw withdrawal threshold, was calculated for each mouse and presented.

2.5. Tissue preparation

Following behavioral tests, mice were processed for immunohistochemistry. Groups tested on day 7 were euthanized on day 8. Groups tested on day 14 were euthanized day 14. BCB mice tested on day 17 were euthanized on day 17. SNPC and PSNL mice tested on day 17 or 21 were euthanized on day 21. Six naïve mice, nine weeks old, were also processed for immunohistochemistry.

Under anesthesia with Zoletil mix-50, 2 μl/g body weight, the mice were fixated by perfusion with 15 ml PBS followed by 40 ml 4% paraformaldehyde (PFA), 7 ml/min (Bie & Berntsen). Spinal cords (segment L4-L6 from PSNL and SNPC mice; L1-L3 or T1-C3 from BCB mice) were isolated, post fixed in 4% PFA over night, cryoprotected overnight in 30% sucrose and fast frozen in OCT compound on a bath of ethanol and dry ice. Bones were isolated from BCB mice, post fixed overnight in 4% PFA and stored in PBS + 0.1% PFA + 0.1% NaN_3 until micro computed tomography (μCT) scannings had been performed.

2.6. Micro-CT

To quantify bone volume fraction (BV/TV), the right distal femur from each BCB mouse was scanned with a high resolution μCT system (vivaCT 40, Scanco Medical AG., Bassersdorf, Switzerland). The scanning resulted in three-dimensional (3D) reconstruction of cubic voxel sizes $25 * 25 * 25\ \mu m^3$, and each 3D image dataset consisted of approximately 210 μCT slide images. 100 slice images (2500 μm) were used for the analysis of subchondral bone tissues (1024×1024 pixels) with 16-bit-gray-levels. BV/TV was computed based on the bone voxel size and the total number of segmented voxels in the 3D image, i.e. bone voxel per total specimen voxel (Ding et al., 1999).

2.7. Immunohistochemistry

Spinal cords were cut at 30 μm on a cryomicrotome and stained as free floating sections. Briefly, sections were collected in PBS + 0.1% Triton X-100 PBS (TPBS) and OCT compound was removed by thorough washing with TPBS followed by incubation for 1 h in TPBS at room temperature (RT). For SP, Iba-1 and GFAP stainings, sections were blocked in BSA/TPBS for 2 h at RT and then incubated overnight in primary antibodies at 4 °C. The following primary antibodies were used: rabbit anti SP (Chemicon AB1566 1:500 in 0.3% BSA/TPBS), rabbit anti Iba-1 (Wako 019-19741 1:1000 in 1% BSA/TPBS) and rabbit anti GFAP (Dako Z0334 1:500 in 2% BSA/TPBS). Next, sections were washed 3 × 5 min in TPBS and incubated in fluorescein isothiocyanate (FITC)-conjugated anti rabbit IgG (Santa Cruz SC-9020) or Alexa 594 anti rabbit IgG (Invitrogen, A31632, 1:300 in BSA/TPBS) for 2 h at RT. Finally, the sections were washed 3 × 5 min in TPBS and mounted on precoated slides (Menzel-Glaser, SuperFrost plus) with permafluor (Thermo, 434990). Stained sections were evaluated with a Zeiss Axioskop 2. The number of Iba-1 positive cells, in spinal cord lamina 1–3 was manually counted. GFAP staining intensity was scored on a continuous and linear scale from 0 to 4 by a trained and blinded observer. At least 10 sections from each mouse were used. SP staining intensity was measured using Image J freeware (National Institute of Health, USA) on 8 bit grey scale pictures obtained with a Hamamatsu C4742 CCD camera using a 10 × Achromat objective and a Zeiss Axioskop 2. The area of SP immunostaining and the mean staining intensity following background correction of the superficial dorsal horn were measured. Integraded staining values defined as area in mm^2 × mean intensity are presented. Presented pictures were captured with either a Zeiss Axioskop 2 combined with a Hamamatsu C4742 CCD camera and a 10 × Achromat objective or with a Nikon Eclipse E100M coupled to a Nikon Photo Head V-TP using a Nikon PanFluor 4 × objective. For OX-42 staining, sections were blocked in 4% donkey serum for 2 h and incubated in rat anti OX-42 (Bioscience, 14-0112-85, 1:100 in 4% donkey serum TPBS) over night. Next, the sections were washed 3 × 5 min in TPBS and incubated 1 h in biotin coupled goat anti rat (DakoCytomation, E0468), washed 3 × 5 min in TPBS and incubated 1 h in HRP coupled streptavidin (DakoCytomation, K3954). Sections were washed 3 × 5 min and exposed to NovaRED (Vektor, SK-4800) for 10 min and washed in normal water. Sections were mounted with Pertex and pictures captured using an Olympus B × 51 microscope and VisioPharm superimage software. At least 3 mice from each group and time point were analysed. A minimum of 10 sections from each mouse were used.

2.8. Statistics

All data were analyzed with one-way ANOVA and Newman Keuls post tests. $P < 0.05$ were set as the threshold of significance. All data are presented as means ± SEM. For behavioral data, all animal groups were compared to the pretest group. For staining data, all groups were compared to tissues originating from naïve mice, except for SP staining analyses where the side ipsilateral to surgery was compared to the contralateral side.

3. Results

3.1. Behavioral tests

Following surgeries, animal pain behavior was evaluated for up to 21 days. To make sure that cancer growth in BCB mice would not result in fractures or penetrate the bone and spread to the surrounding muscle tissue, BCB mice were euthanized on day 17.

At day 7 post surgery, BCB mice expressed tactile hypersensitivity which was augmented on day 14 and 17. These mice also expressed a decrease in limb use over time that was found to be significant at day 14 and 17 (Fig. 1b). In contrast, SNPC mice did not express tactile hypersensitivity at day 7 but had developed tactile hypersensitivity at day 14. However, from day 14 to day 21 these mice seemed to loose sensitivity and also developed foot-drop which is a sign of compromised nerve function (Fig. 1a). A decrease in limb use over time was also observed but not to the extend seen in the BCB mice (Fig. 1b). As previously reported, PSNL mice were hypersensitive to tactile stimuli on all test days (7, 14 and 21 post surgery). However, the hypersensitivity never reached the levels observed in the two cancer pain models (Fig. 1a). As PSNL operations involve direct damage of the motor neurons projecting to the leg, limb use tests of these animals were not performed.

3.2. Bone destruction

The extend of tumor induced bone destruction of the distal femoral bone of BCB mice was assessed by μCT scanning. Bone cancer growth led to a progressive loss of bone tissue and at day 17 the BV/TV index of the distal femoral bone was decreased to 36% (Fig. 2). However, at this point there were no visible signs of tumor growth outside of the bones. The degree of bone destruction was found to correlate with tactile hypersensitivity ($r = 0.73$, $p < 0.001$) and to decreased limb use ($r = 0.71$, $p < 0.001$).

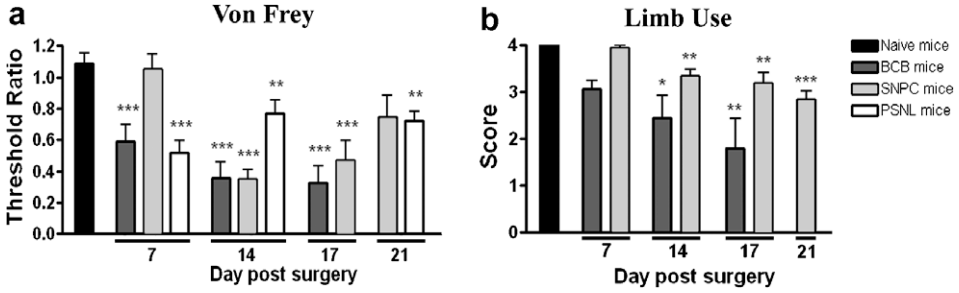

Fig. 1. Pain behavior of BCB, SNPC and PSNL mice. (a) Tactile sensitivity of BCB, SNPC and PSNL mice compared to naïve mice. BCB mice expressed tactile hypersensitivity determined by von Frey tests on all test days. SNPC mice expressed tactile hypersensitivity at day 14 but at later time points a progressive loss of planter sensation was evident. PSNL mice expressed tactile hypersensitivity from day 7 to 21. (b) Voluntary limb use of BCB, SNPC and PSNL mice compared with naïve mice. For BCB mice, a decrease in limb use became significant at day 14 post surgery. The SNPC mice also expressed a steady decline in limb use over time. Data represents mean ± SEM. Compared to naïve mice *, $p < 0.05$; **, $p < 0.01$; ***, $p < 0.001$. Data was analyzed with one way ANOVA with a Newman Keuls post test. For naïve, BCB, SNPC and PSNL mice each time point represents at least 10, 8, 10 and 6 mice, respectively.

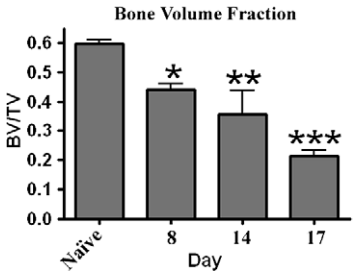

Fig. 2. Progressive bone loss in BCB mice over time. Bone volume fractions were determined by μCT and found to decrease compared to naïve mice already 7 days post cancer inoculation. Bone volume fraction of the distal femoral bone further decreased over time to reach values of 35% of naïve mice on day 17. Data represents mean ± SEM. Compared to pretest values *, $p < 0.05$; **, $p < 0.01$; ***, $p < 0.001$. Data was analyzed with one way ANOVA with a Newman Keuls post test. $n = 5, 5, 4, 4$ for pretest, day 7, 14 and 17, respectively.

3.3. Spinal SP levels

One hallmark of injured sensory nerves is decreased levels of spinal SP at distinct time points following the injury. Spinal SP levels were investigated in the PSNL mice and found to be decreased at day 7 ipsilateral to the operation side when compared to the contralateral side. A further decrease was observed at day 14. However, at day 21, SP levels seemed to approach basal levels again. During this timecourse, no variations were found in the contralateral side (Fig. 3a and b). These findings corroborates previous reports on spinal SP expression in this model (Inoue et al., 2006; Malmberg and Basbaum, 1998).

3.4. Temporal changes in spinal glia activity

Activation of spinal cord microglia in the three different pain models was investigated by Iba-1 and confirmed by OX-42 immunohistochemistry. PSNL mice showed substantial microglial activation (Fig. 4a), defined as an increase in number and transition into a more rounded morphology, in the superficial dorsal horn as well as lateral in lamina 9. Besides, the whole ipsilateral side of the spinal cord exhibited a subtle increase in the number and staining intensity of Iba-1 positive microglia. At day 21 the number of microglia, in PSNL mice, was reduced to baseline levels (Fig. 4a). No effect on microglial numbers or morphology were observed in the BCB and SNPC mice at any time point (Fig. 4a).

Similar observations were found when staining for the microglial antigen OX-42 (Fig. 5). PSNL mice expressed abundant OX-42 staining ipsilateral compared to contralateral to the injured nerve, both in the dorsal and ventral horn, 8 days post surgery. In contrast BCB mice showed no signs of microglial activation at any time point. However, 8 days post surgery, a very subtle increase in OX-42 staining restricted to the lateral superficial dorsal horn and to the superficial ventral horn was observed SNPC mice. This increase was not evident at day 14 post surgery.

Activation of spinal cord astrocytes was investigated by GFAP immunohistochemistry. In BCB mice, GFAP staining intensity increased at day 8 and it continued to increase over time until day 17, where the entire ipsilateral side expressed an immense presence of GFAP positive cells (Fig. 6). As sham operated mice, in this model, have been reported to express increased levels of spinal GFAP (Sevcik et al., 2004), we investigated the degree of GFAP staining in sham operated mice at the end of the time course.

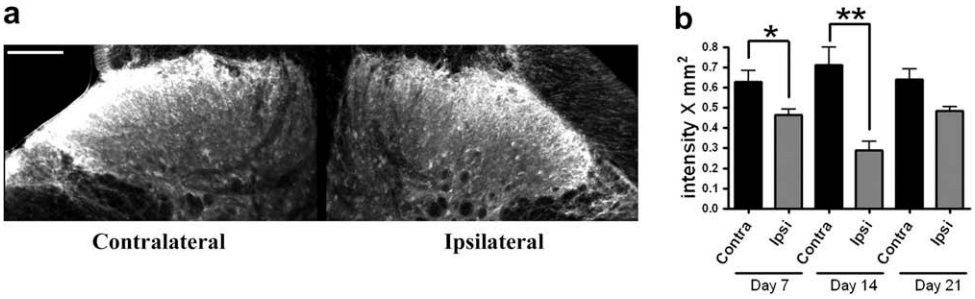

Fig. 3. Decreased spinal SP levels in PSNL mice. (a) Staining intensity of spinal SP in PSNL mice showed that SP levels had decreased in response to nerve injury (representative staining at day 14 post injury). (b) Whole superficial dorsal horn staining intensity was measured after background correction. No difference in SP levels contralateral to the nerve injury was observed at any time point. Ipsilateral to the injury, a transient and significant decrease was seen. Data represents mean ± SEM. *, $p < 0.05$; **, $p < 0.01$. Data was analyzed with one way ANOVA with a Newman Keuls post test. $n = 4, 4, 3$ for day 7, 14 and 21, respectively. Scale bar = 100 μm.

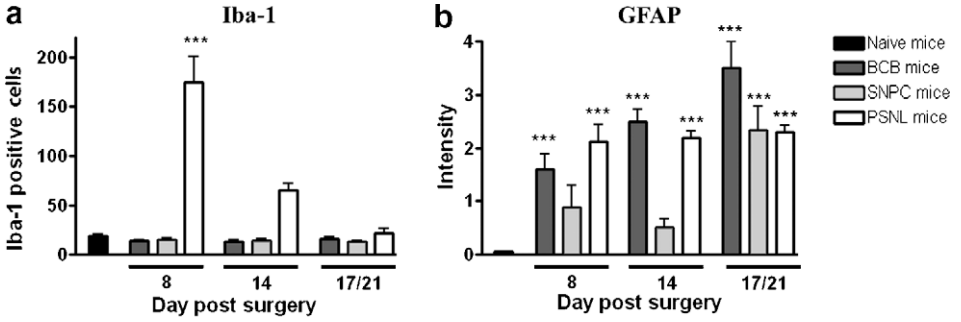

Fig. 4. Number of Iba-1 positive cells with glial morphology and GFAP staining intensity. (a) Spinal cords were stained with Iba-1 antibodies and the number of stained cells were determined ipsilateral to the surgery. PSNL mice expressed an increased presence of microglia, while BCB mice and SNPC mice did not show any alterations. (b) GFAP staining intensity was evaluated ipsilateral to the surgery and scored on a scale from 0 to 4. All three models developed astrogliosis over time but to various degrees. Data represents mean ± SEM. Compared to naïve mice ***, $p < 0.001$. Data was analyzed with one way ANOVA with a Newman Keuls post test. For naïve, BCB, SNPC and PSNL mice each time point represents at least 6, 4, 4, 4, mice respectively.

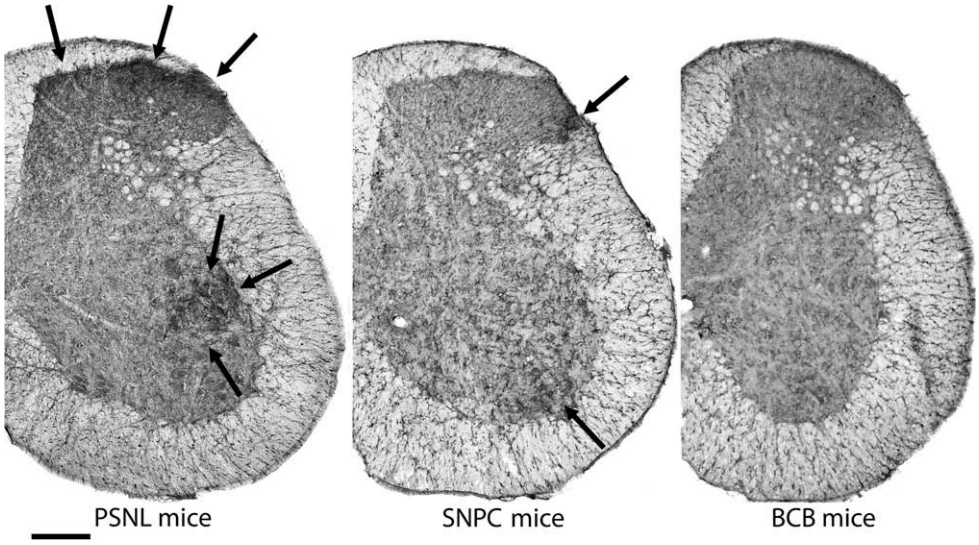

Fig. 5. Spinal expression of OX-42. Spinal cord sections obtained 8 days post surgery and stained with antibodies against the microglial marker OX-42 are presented. Pictures were captured using the Olympus BX51 microscope and VisioPharm superimage software. Arrows indicate areas with increased OX-42 staining. Scale bar = 200 μm.

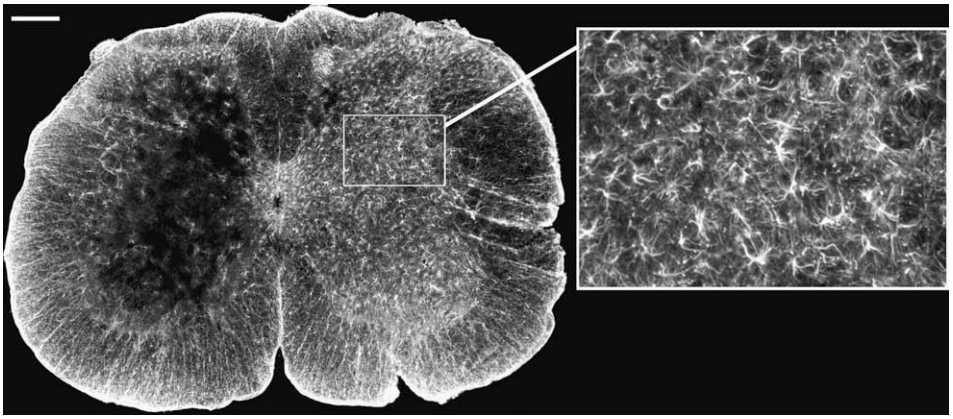

Fig. 6. Widespread spinal astrogliosis in BCB mice. Immunohistochemical staining of spinal GFAP reveals massive astrogliosis in all spinal cord lamina of BCB mice 17 days post surgery. High resolution pictures were constructed by multiple 8 bit picture fragments obtained with the Zeiss Axioskop 2, Hamamatsu C4742 CCD camera and a 10 × Achromat objective. Scale bar = 200 μm.

We found that the GFAP staining intensity in sham operated mice was increased compared to naïve mice but not to the extend found in the BCB mice (data not shown).

SNPC mice expressed a small increase in GFAP staining at day 8 and 14 which was markedly increased at day 21 (Fig. 4b).

PSNL mice expressed increased GFAP staining, which remained constant at all time points examined (Fig. 4b). In the PSNL mice, astrogliosis was most pronounced in areas, which also displayed an increased presence of microglia (Fig. 7).

As SNPC and PSNL sham operated mice do not express any increase in spinal GFAP levels (Coyle, 1998) (personal observations), we did not include these groups in the present study.

3.5. Spread of spinal astrogliosis

Spinal cords derived from BCB mice were divided according to vertebrae entities from T1 to S1 and stained for GFAP. Increased astrogliosis ipsilateral to the cancer bearing limb was observed in spinal cord segments T10–S1. The central part of this segment (T12–L5) showed the most extensive astrogliosis, whereas the astrogliosis decreased in the distal parts until it reached levels similar to that observed in the contralateral side (Fig. 8). No spread of astrogliosis was found in sham operated mice.

4. Discussion

In the present report, we have demonstrated that in pain models astrocyte activation can take place independent of microglial activity, though microglial activation may also lead to secondary astrogliosis in nerve injury pain models. The spread of astrogliosis was examined in BCB mice and astrogliosis was shown to be present in spinal cord segments adjacent to the segments, where the primary afferent neurons innervating the femoral bone, enters the spinal cord.

Spinal cord astrogliosis is a hallmark of chronic pain models, including classical neuropathic and inflammatory models such as PSNL, spinal nerve ligation, sciatic nerve transection, bone cancer pain as well as complete Freund's adjuvant (CFA), formalin and zymosan injection (Colburn et al., 1999; Honore et al., 2000; Medhurst et al., 2002; Raghavendra et al., 2004; Sweitzer et al., 1999) which indicates that spinal astrogliosis is inevitable following an insult that leads to sustained nociceptive signaling to the CNS

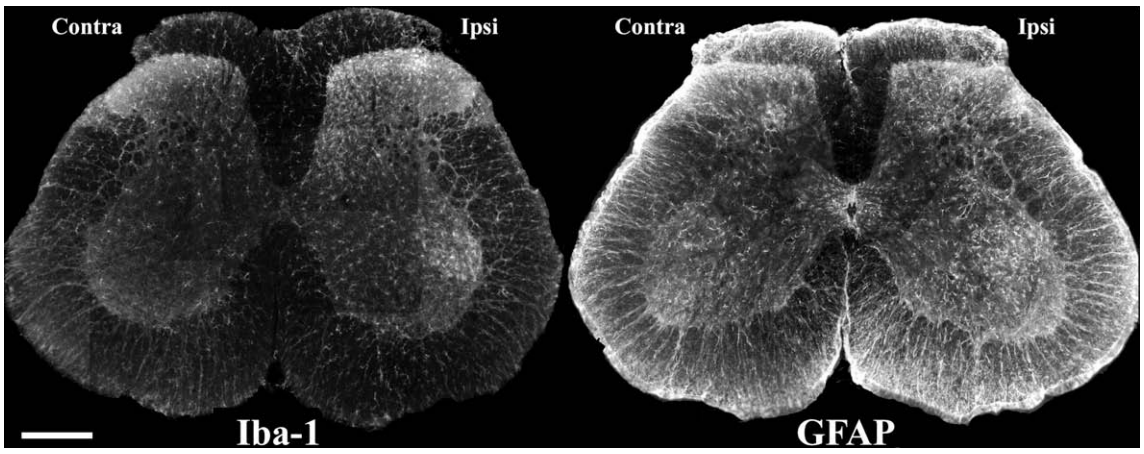

Fig. 7. Spinal cord GFAP and Iba-1 staining of PSNL mice. GFAP and Iba-1 staining of spinal cord sections from PSNL mice revealed increased levels of both GFAP and Iba-1 positive cells. Increased numbers of Iba-1 positive cells were most pronounced in the superficial dorsal horn and superficial ventral horn (lamina 9) though the entire side of the spinal cord ipsilateral to the nerve ligation exhibited a higher staining intensity of the individual Iba-1 positive cell. GFAP staining was, in contrast to BCB and SNPC mice, restricted to spinal cord areas which also express increased levels of Iba-1 positive cells. The presented sections were derived from PSNL mice 14 days post surgery. Scale bar = 300 μm.

and could be expected to be found in other models involving high and persistent sensory activity.

Von Frey tests of SNPC mice, showing first an increase (day 14) and thereafter a decrease in tactile hypersensitivity is in agreement with data presented by Shimoyama et al. (2005), where both tactile and thermal sensitivity was lacking 18 days post cancer inoculation. In spite of the lost sensitivity they showed that SNPC mice still experienced pain by use of flinch tests and spinal upregulation of Fos, a marker of neuronal activity (Coggeshall, 2005; Shimoyama et al., 2005). The loss of sensation following a period of hypersensitivity in these mice is likely accounted for by compression of the sciatic nerve by the growing tumor. This would also explain the foot-drop tendency, a symptom observed in humans with compromised function of the sciatic nerve.

The findings that astrogliosis in the BCB and SNPC mice occurs independent of microglial activation suggest that astrocytes are activated as a direct consequence of neuronal activity. This would also explain why inflammatory pain in rats could lead to a 300% GFAP upregulation already after 30 min (Guo et al., 2007). A link between neuronal activity and GFAP expression is supported by the findings that electrical induced seizures lead to increased GFAP gene transcription not only in the directly affected brain areas but also in synaptically associated brain areas (Steward et al., 1991). Furthermore, in an inflammatory pain model, astrogliosis has been shown to be abrogated by a nerve blockade with lidocaine thereby emphasizing the importance of neuronal signal transduction for astrocyte activation (Guo et al., 2007). Though several nerve derived factors such as glutamate, SP, CGRP, NO and ATP have the potential to activate astrocytes in vitro, their contribution in astrocyte activation in vivo is still unresolved. Besides neurotransmitters, other factors, such as potassium released from firing neurons have the potential to activate astrocytes. Furthermore, cytokines released from tumors might indirectly sensitize the spinal cord astrocytes (Hansson, 2006).

Sensitivity tests of the affected nerves in the two cancer pain models are hampered by the model design. In the case of SNPC mice, the present study shows, that sciatic nerve compression by the tumor results in loss of sensitivity after a period with plantar hypersensitivity. However, spinal Fos staining shows that SNPC mice still experience chronic nociceptive signaling regardless of the loss of plantar sensitivity (Shimoyama et al., 2005). In BCB mice the direct affected nerve proves difficult to test by application of stimuli to the skin. However, in these two cancer pain models, where astrocytes are likely activated through neuronal activity and not by activated microglia, GFAP could possibly be used as a neurochemical marker of nociception.

The findings that astrogliosis was restricted to areas with increased microglial activity in some of the PSNL mice, suggest a connection between these two phenomena in this model. Though the exact nature of microglial derived astrocyte activators, in regard to pain pathology, remains unknown, combinations of transmitters, which can be released by activated microglia, such as TNF-α, IL-1β and NO have been shown, in related research fields, to stimulate astrocyte activation (Brahmachari et al., 2006; Falsig et al., 2004; Lund et al., 2006).

An interesting phenomenon in BCB mice is the presence of plantar hypersensitivity which reflects changes in nociceptive signal transduction by the sciatic nerve to higher brain centers. How bone cancer affecting the femoral nerve leads to plantar hypersensitivity is not yet known but could result from heterosynaptic sensitization of spinal cord neurons (Ji et al., 2003). However, peripheral mechanisms may also be involved as the dorsal root ganglia (DRG) containing the cell bodies of the femoral bone innervating neurons (L1–L3) also to a limited extend contain neurons which make up part of the sciatic nerve (Peters et al., 2005). In response to femoral bone cancer, these DRG express an increased presence of macrophages and satellite cells (Peters et al., 2005) which could produce diffusible substances that could sensitize surrounding neurons (Hanani, 2005; Ma and Quirion, 2005). The tomographic examination of BCB mice, presented in this report, showed that astrogliosis was evident from spinal cord segment T10–S1. The nerves that innervate the femoral bone enters the spinal cord in segment L1–L3 (Peters et al., 2005) meaning that astrogliosis had spread into distant spinal cord segments both caudally and rostrally from that area. Astrogliotic spread may reflect the collateral arborizations of dorsal root fibers in the spinal cord (Shortland and Wall, 1992) but it could also result from signal transduction from the site of primary afferent entrance to adjacent spinal cord segments by intersegmental propriospinal neurons (Almeida et al., 2004). The ability of astrocytes to construct networks, which are capable of transmitting signals for long distances and which result in the secretion of substances that can induce astrocyte differentiation and proliferation, could also be involved in generation of astrogliotic spread (Faijerson et al., 2006; Franke et al., 1999; Haydon, 2001).

As both hypersensitivity related to distinct spinal cord segments and astrogliosis is found to spread along the spinal cord

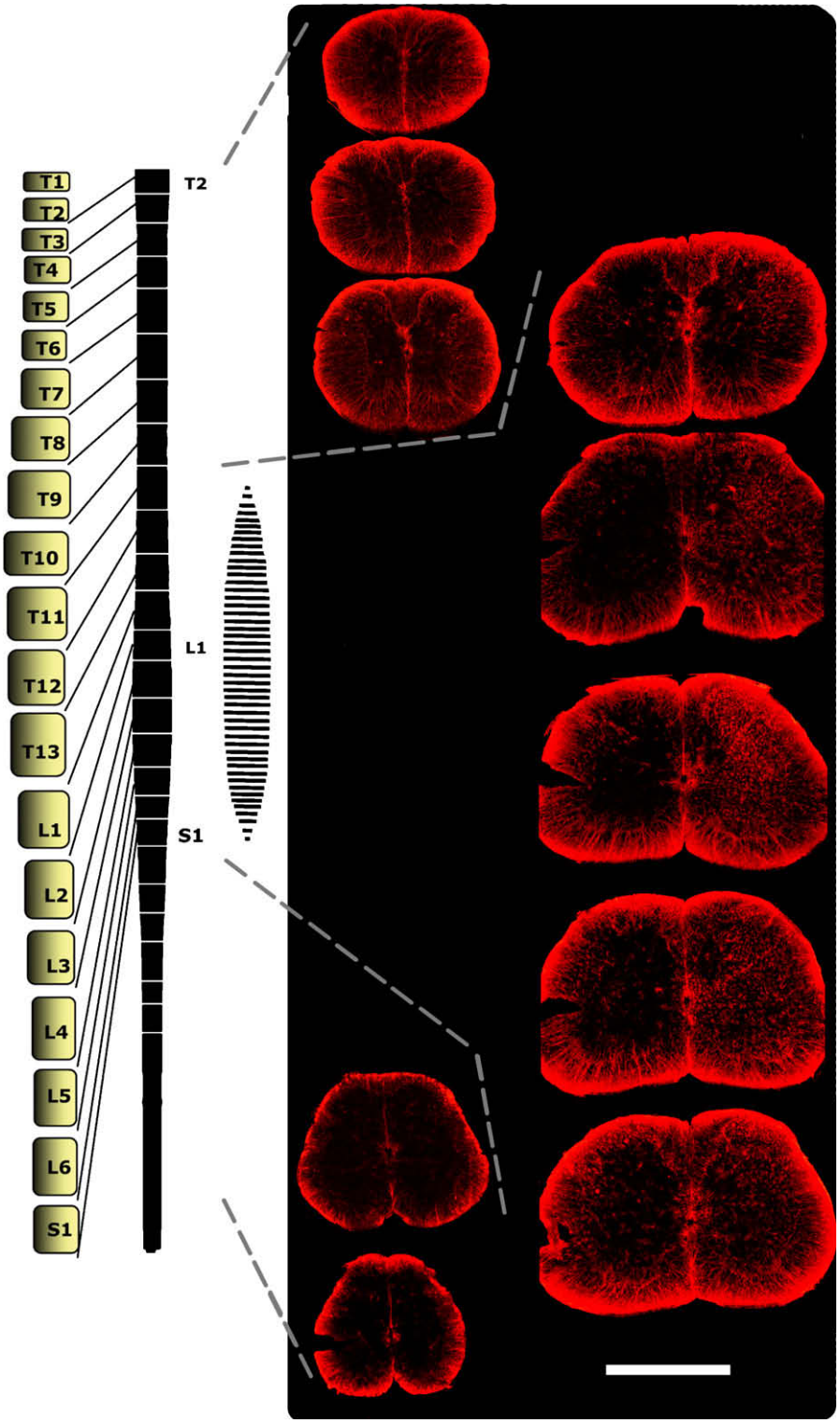

Fig. 8. Spread of spinal astrogliosis in BCB mice. 6 BCB mice, which had developed significant and severe pain behavior (Limb use $\leqslant$1), and 3 sham mice were used to investigate the spread of spinal astrogliosis. Spinal vertebrates with designations are shown on the left. Nerve roots projecting from the spinal cord to their respective DRG are shown between the vertebrates and the spinal cord (spinal cord segments T2, L1 and S1 are marked). Just on the right hand side of the spinal cord is the degree of spinal astrogliosis marked by horizontal fine lines. On the right hand side of the diagram are representative spinal cord GFAP stainings from various spinal cord segments. Scale bar = 1000 μm.

these two phenomena may be interrelated. In that case, the spread of hypersensitivity could be the primary event which, in turn, triggered astrogliosis but the spread of astrogliosis could also lead to spread of hypersensitivity as astrocytes are known to modulate neuronal signal transduction (Volterra and Meldolesi, 2005).

In the present report, we have shown that astrogliosis is a common hallmark in three different pathological pain models and that it can take place independent of microglial activation thus proving the presence of discriminative mechanisms behind microglial and astrocytic activation in pain models. As spinal astrogliosis in the

cancer pain models may reflect the degree of neuronal activity GFAP could possibly be used as a marker for the duration and severity of pain in these models. Furthermore, the observed spread of astrogliosis in BCB mice offers an explanation of how hyperalgesia may spread to areas not related to the primary source of pain, though the opposite situation, where a spread of hypersensitivity activates astrocytes adjacent to the primarily activated astrocytes, should not be ruled out. The factors leading to astrocyte activation in pain models still remain unidentified, though several nerve derived factors have been proposed. How astrocytes may facilitate pain transmission has yet to be finally elucidated.

Acknowledgements

We would like to thank Kirsten Jørgensen, Pia Møller Carstensen, Lone Helboe and Julie Lotharius at Department of Neurobiology, H. Lundbeck A/S, Denmark for their kind help with histological procedures and use of the Nikon microscopy equipment. We would also like to thank Kirsten Metz from the Faculty of Pharmaceutical Sciences, Copenhagen University for technical assistance.

References

Almeida TF, Roizenblatt S, Tufik S. Afferent pain pathways: a neuroanatomical review. Brain Res 2004;1000:40–56.
Baron R. Mechanisms of disease: neuropathic pain – a clinical perspective. Nat Clin Pract Neurol 2006;2:95–106.
Brahmachari S, Fung YK, Pahan K. Induction of glial fibrillary acidic protein expression in astrocytes by nitric oxide. J Neurosci 2006;26:4930–9.
Coggeshall RE. Fos, nociception and the dorsal horn. Prog Neurobiol 2005;77:299–352.
Colburn RW, Rickman AJ, DeLeo JA. The effect of site and type of nerve injury on spinal glial activation and neuropathic pain behavior. Exp Neurol 1999;157:289–304.
Coull JA, Beggs S, Boudreau D, Boivin D, Tsuda M, Inoue K, et al. BDNF from microglia causes the shift in neuronal anion gradient underlying neuropathic pain. Nature 2005;438:1017–21.
Coyle DE. Partial peripheral nerve injury leads to activation of astroglia and microglia which parallels the development of allodynic behavior. Glia 1998;23:75–83.
Ding M, Odgaard A, Hvid I. Accuracy of cancellous bone volume fraction measured by micro-CT scanning. J Biomech 1999;32:323–6.
Faijerson J, Tinsley RB, Aprico K, Thorsell A, Nodin C, Nilsson M, et al. Reactive astrogliosis induces astrocytic differentiation of adult neural stem/progenitor cells in vitro. J Neurosci Res 2006;84:1415–24.
Falsig J, Latta M, Leist M. Defined inflammatory states in astrocyte cultures: correlation with susceptibility towards CD95-driven apoptosis. J Neurochem 2004;88:181–93.
Franke H, Krugel U, Illes P. P2 receptor-mediated proliferative effects on astrocytes in vivo. Glia 1999;28:190–200.
Garrison CJ, Dougherty PM, Carlton SM. GFAP expression in lumbar spinal cord of naive and neuropathic rats treated with MK-801. Exp Neurol 1994;129:237–43.
Garrison CJ, Dougherty PM, Kajander KC, Carlton SM. Staining of glial fibrillary acidic protein (GFAP) in lumbar spinal cord increases following a sciatic nerve constriction injury. Brain Res 1991;565:1–7.
Guo W, Wang H, Watanabe M, Shimizu K, Zou S, LaGraize SC, et al. Glial-cytokine-neuronal interactions underlying the mechanisms of persistent pain. J Neurosci 2007;27:6006–18.
Hains BC, Waxman SG. Activated microglia contribute to the maintenance of chronic pain after spinal cord injury. J Neurosci 2006;26:4308–17.
Hald A, Lotharius J. Oxidative stress and inflammation in Parkinson's disease: is there a causal link? Exp Neurol 2005;193:279–90.
Hanani M. Satellite glial cells in sensory ganglia: from form to function. Brain Res Brain Res Rev 2005;48:457–76.
Hansson E. Could chronic pain and spread of pain sensation be induced and maintained by glial activation? Acta Physiol (Oxf) 2006;187:321–7.
Haydon PG. GLIA: listening and talking to the synapse. Nat Rev Neurosci 2001;2:185–93.
Honore P, Rogers SD, Schwei MJ, Salak-Johnson JL, Luger NM, Sabino MC, et al. Murine models of inflammatory, neuropathic and cancer pain each generates a unique set of neurochemical changes in the spinal cord and sensory neurons. Neuroscience 2000;98:585–98.
Inoue M, Yamaguchi A, Kawakami M, Chun J, Ueda H. Loss of spinal substance P pain transmission under the condition of LPA1 receptor-mediated neuropathic pain. Mol Pain 2006;2:25.
Ji RR, Kohno T, Moore KA, Woolf CJ. Central sensitization and LTP: do pain and memory share similar mechanisms? Trends Neurosci 2003;26:696–705.
Lazar P, Reddington M, Streit W, Raivich G, Kreutzberg GW. The action of calcitonin gene-related peptide on astrocyte morphology and cyclic AMP accumulation in astrocyte cultures from neonatal rat brain. Neurosci Lett 1991;130:99–102.
Lee Y, Lee CH, Oh U. Painful channels in sensory neurons. Mol Cells 2005;20:315–24.
Lin CS, Tsaur ML, Chen CC, Wang TY, Lin CF, Lai YL, et al. Chronic intrathecal infusion of minocycline prevents the development of spinal-nerve ligation-induced pain in rats. Reg Anesth Pain Med 2007;32:209–16.
Lund S, Christensen KV, Hedtjarn M, Mortensen AL, Hagberg H, Falsig J, et al. The dynamics of the LPS triggered inflammatory response of murine microglia under different culture and in vivo conditions. J Neuroimmunol 2006;180:71–87.
Ma W, Quirion R. Up-regulation of interleukin-6 induced by prostaglandin E from invading macrophages following nerve injury: an in vivo and in vitro study. J Neurochem 2005;93:664–73.
Malmberg AB, Basbaum A. I. Partial sciatic nerve injury in the mouse as a model of neuropathic pain: behavioral and neuroanatomical correlates. Pain 1998;76:215–22.
Medhurst SJ, Walker K, Bowes M, Kidd BL, Glatt M, Muller M, et al. A rat model of bone cancer pain. Pain 2002;96:129–40.
Neary JT, Baker L, Jorgensen SL, Norenberg MD. Extracellular ATP induces stellation and increases glial fibrillary acidic protein content and DNA synthesis in primary astrocyte cultures. Acta Neuropathol (Berl) 1994;87:8–13.
Noble LJ, Hall JJ, Chen S, Chan PH. Morphologic changes in cultured astrocytes after exposure to glutamate. J Neurotrauma 1992;9:255–67.
Park YK, Chung YS, Kim YS, Kwon OY, Joh TH. Inhibition of gene expression and production of iNOS and TNF-alpha in LPS-stimulated microglia by methanol extract of Phellodendri cortex. Int Immunopharmacol 2007;7:955–62.
Peters CM, Ghilardi JR, Keyser CP, Kubota K, Lindsay TH, Luger NM, et al. Tumor-induced injury of primary afferent sensory nerve fibers in bone cancer pain. Exp Neurol 2005;193:85–100.
Raghavendra V, Tanga F, DeLeo JA. Inhibition of microglial activation attenuates the development but not existing hypersensitivity in a rat model of neuropathy. J Pharmacol Exp Ther 2003;306:624–30.
Raghavendra V, Tanga FY, DeLeo JA. Complete Freunds adjuvant-induced peripheral inflammation evokes glial activation and proinflammatory cytokine expression in the CNS. Eur J Neurosci 2004;20:467–73.
Schwei MJ, Honore P, Rogers SD, Salak-Johnson JL, Finke MP, Ramnaraine ML, et al. Neurochemical and cellular reorganization of the spinal cord in a murine model of bone cancer pain. J Neurosci 1999;24:10886–97.
Sevcik MA, Luger NM, Mach DB, Sabino MA, Peters CM, Ghilardi JR, et al. Bone cancer pain: the effects of the bisphosphonate alendronate on pain, skeletal remodeling, tumor growth and tumor necrosis. Pain 2004;111:169–80.
Shimoyama M, Tatsuoka H, Ohtori S, Tanaka K, Shimoyama N. Change of dorsal horn neurochemistry in a mouse model of neuropathic cancer pain. Pain 2005;114:221–30.
Shortland P, Wall PD. Long-range afferents in the rat spinal cord II. Arborizations that penetrate grey matter. Philos Trans R Soc Lond B Biol Sci 1992;337:445–55.
Steward O, Torre ER, Tomasulo R, Lothman E. Neuronal activity up-regulates astroglial gene expression. Proc Natl Acad Sci USA 1991;88:6819–23.
Sweitzer SM, Colburn RW, Rutkowski M, DeLeo JA. Acute peripheral inflammation induces moderate glial activation and spinal IL-1beta expression that correlates with pain behavior in the rat. Brain Res 1999;829:209–21.
Volterra A, Meldolesi J. Astrocytes, from brain glue to communication elements: the revolution continues. Nat Rev Neurosci 2005;6:626–40.